High-pressure study of lithium amidoborane using Raman spectroscopy and insight into dihydrogen bonding absence

Shah Najiba[a,1] and Jiuhua Chen[a,b,1]

[a]Center for the Study of Matter at Extreme Conditions, Department of Mechanical and Materials Engineering, Florida International University, Miami, FL 33199; and [b]Center for High Pressure Science and Technology Advanced Research, Beijing 100088, China

Edited* by Ho-kwang Mao, Carnegie Institution of Washington, Washington, DC, and approved September 27, 2012 (received for review July 4, 2012)

One of the major obstacles to the use of hydrogen as an energy carrier is the lack of proper hydrogen storage material. Lithium amidoborane has attracted significant attention as hydrogen storage material. It releases ∼10.9 wt% hydrogen, which is beyond the Department of Energy target, at remarkably low temperature (∼90 °C) without borazine emission. It is essential to study the bonding behavior of this potential material to improve its dehydrogenation behavior further and also to make rehydrogenation possible. We have studied the high-pressure behavior of lithium amidoborane in a diamond anvil cell using in situ Raman spectroscopy. We have discovered that there is no dihydrogen bonding in this material, as the N—H stretching modes do not show redshift with pressure. The absence of the dihydrogen bonding in this material is an interesting phenomenon, as the dihydrogen bonding is the dominant bonding feature in its parent compound ammonia borane. This observation may provide guidance to the improvement of the hydrogen storage properties of this potential material and to design new material for hydrogen storage application. Also two phase transitions were found at high pressure at 3.9 and 12.7 GPa, which are characterized by sequential changes of Raman modes.

Hydrogen economy has been considered as potentially efficient and environmental friendly alternative energy solution (1). However, one of the most important scientific and technical challenges facing the "hydrogen economy" is the development of safe and economically viable on-board hydrogen storage for fuel cell applications, especially to the transportation sector. Ammonia borane (BH_3NH_3), a solid state hydrogen storage material, possesses exceptionally high hydrogen content (19.6 wt%) and in particular, it contains a unique combination of protonic and hydridic hydrogen, and on this basis, offers new opportunities for developing a practical source for generating molecular dihydrogen (2–5). Stepwise release of H_2 takes place through thermolysis of ammonia borane, yielding one-third of its total hydrogen content (6.5 wt%) in each heating step, along with emission of toxic borazine (6–8). Recently, research interests are focusing on how to improve discharge of H_2 from ammonia borane, including lowering the dehydrogenation temperature and enhancing hydrogen release rate using different techniques, e.g., nanoscaffolds (9), ionic liquids (10), acid catalysis (11), base metal catalyst (12), or transition metal catalysts (13, 14). More recently, significant attention is given to chemical modification of ammonia borane through substitution of one of the protonic hydrogen atoms with an alkali or alkaline–earth element (15–21). Lithium amidoborane ($LiNH_2BH_3$) has been successfully synthesized by ball milling LiH with NH_3BH_3 (15–18). One of the driving forces suggested for the formation of $LiNH_2BH_3$ is the chemical potential of the protonic $H^{\delta+}$ in NH_3 and the hydridic $H^{\delta-}$ in alkali metal hydrides making them tend to combine, producing H_2 + $LiNH_2BH_3$. $LiNH_2BH_3$ exhibits significantly different and improved dehydrogenation characteristics from its parent compound ammonia borane. It releases more than 10 wt% of hydrogen at around 90 °C without borazine emission. Also, the dehydrogenation process of lithium amidoborane is much less exothermic (∼3–5 kJmole^{-1} H_2) (15–17) than that of NH_3BH_3 (∼22.5 kJmole^{-1} H_2) (6–8), which greatly enhances the search for suitable regeneration routes (prerequisite for a hydrogen storage material). Although the rationale behind the improved dehydrogenation behavior is still unclear, these improved property modifications evidently originate from the substitution of one H in the NH_3 group by the more electron-donating Li, which exerts influences on the bonding characteristics, especially on the dihydrogen bonding, which is one of the characteristic bonds of ammonia borane (15). So, it is essential to understand details about the bonding behavior of this potential material.

High-pressure study of molecular crystals can provide unique insight into the intermolecular bonding forces, such as hydrogen bonding and phase stability in hydrogen storage materials and thus provides insight into the improvement of design (22–30). For instance, Raman spectroscopic study of ammonia borane at high pressure provided insight about its phase transition behavior and the presence of dihydrogen bonding in its structure (25–30). We have investigated $LiNH_2BH_3$ at high pressure using Raman spectroscopy. We have found that, other than in NH_3BH_3, dihydrogen bonding is absent in lithium amidoborane structure and $LiNH_2BH_3$ shows two phase transitions at high pressure.

Results and Discussion

We have used in situ Raman spectroscopy to characterize bonding changes in the sample. For collecting the Raman spectra at ambient condition, we have loaded ammonia borane and lithium amidoborane samples into glass capillaries. Raman spectra (Fig. 1) of ammonia borane (25–30) and lithium amidoborane (31) at ambient condition have been well documented, and the major Raman modes can be described by their molecular nature: N—H stretching, B—H stretching, and B—N stretching modes. In the Raman spectra, B—H stretching modes of lithium amidoborane appear at lower wavenumbers compared with those of ammonia borane (Fig. 1), indicating that lithium amidoborane has weaker B—H bond than ammonia borane. This observation is consistent with the reported B—H bond strength by the previous X-ray studies (15, 18, 31–34). Likewise, both the N—H and B—N stretching modes in lithium amidoborane appear at higher wavenumbers with respect to those in ammonia borane, i.e., the N—H and B—N bonds become stronger in lithium amidoborane, consistent with the prediction by Armstrong et al. regarding B—N bond strength (35).

We have conducted diamond anvil cell (DAC) experiments at room temperature on a lithium amidoborane sample from ambient pressure to 19 GPa. Two phase transformations are

Author contributions: S.N. and J.C. designed research; S.N. and J.C. performed research; S.N. analyzed data; and S.N. and J.C. wrote the paper.

The authors declare no conflict of interest.

*This Direct Submission article had a prearranged editor.

[1]To whom correspondence may be addressed. E-mail: snaji001@fiu.edu or chenj@fiu.edu.

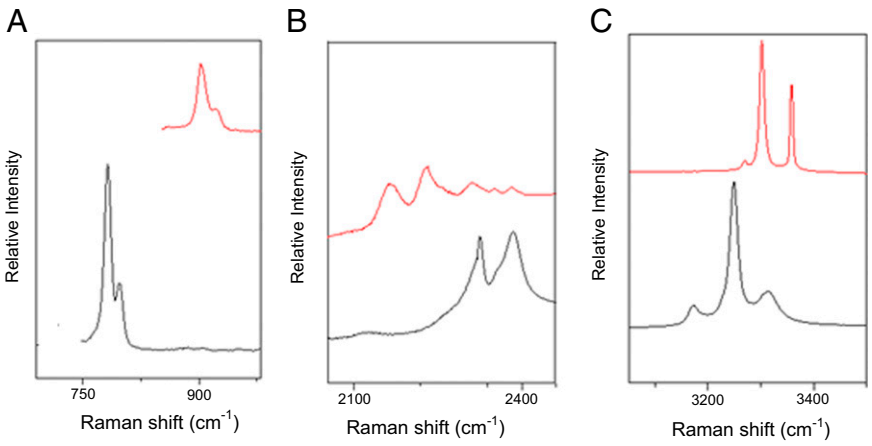

Fig. 1. Comparison of the major Raman modes of ammonia borane (black line) and lithium amidoborane (red line) B—N (*A*), B—H (*B*), and N—H (*C*) stretching modes.

observed at high pressure. The first phase transition occurs at 3.9 GPa. This phase transformation is demonstrated by remarkable change in the B—H stretching region. The low-frequency B—H stretching mode splits and the high frequency B—H stretching modes merge into singlet (Fig. 2*A*). Also, a notable change in optical image occurs at this phase transition. The sample is opaque

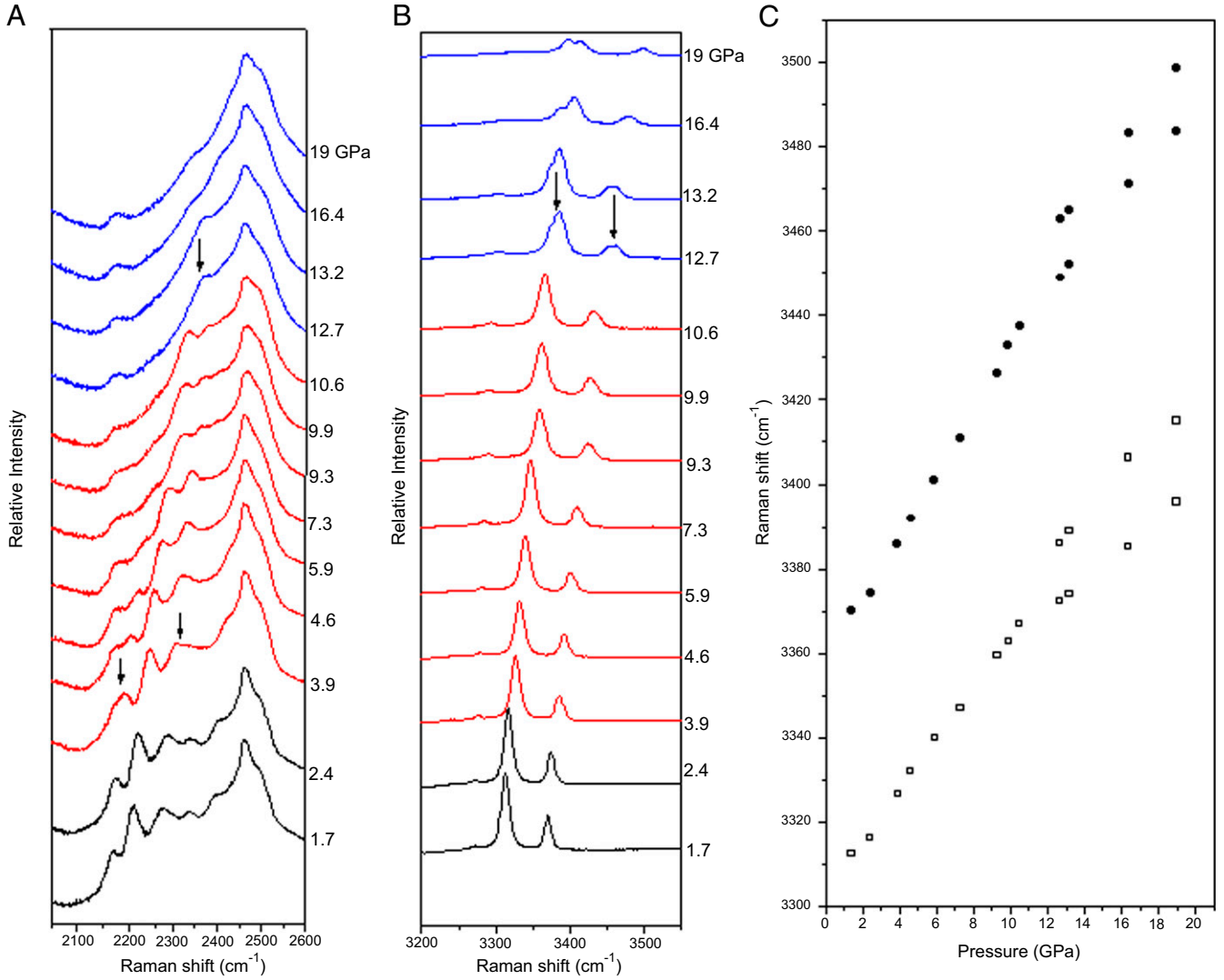

Fig. 2. Evolution of N—H and B—H stretching modes at high pressure: B—H (*A*) and N—H (*B*) stretching modes, arrow (↓) indicates the position of merging and/or splitting of Raman modes. (*C*) Pressure dependence of Raman shift of N—H stretching modes.

to light before phase transformation and is transparent to light after phase transformation (Fig. 3). With further compression, another phase transition occurs at 12.7 GPa, with the clear splitting of N—H stretching vibrational modes and merging of high frequency B—H stretching modes (Fig. 2 *A*–*C*). Both phase transitions are associated with splitting of the major vibrational modes indicating that the structural complexity increases with pressure.

The characteristic feature in the structure of ammonia borane is that due to the differing electronegativities of the B and N atoms, the hydrogen atoms bonded respectively to B and N have different charges. As nitrogen is strongly electronegative, the hydrogens bonded to nitrogen are protonic ($H^{\delta+}$) in character; whereas boron is less electronegative than hydrogen and thus the hydrogens bonded to boron are hydridic ($H^{\delta-}$) in character. These two hydrogen species form a network of N—$H^{\delta+}$...$^{-\delta}$H—B dihydrogen bonds, which stabilize the structure of NH_3BH_3 as molecular solid with much higher melting point (+104 °C) compared with the isoelectronic CH_3CH_3 (melting point is −181 °C) gas and most importantly, the existence of these dihydrogen bonds facilitates the formation of molecular hydrogen during dehydrogenation of ammonia borane. In fact, formation or strengthening of such dihydrogen bonds results in weakening of N—H bonds and therefore a corresponding red shift of N—H stretching frequency to lower wavenumbers in Raman spectra (36). For example, the frequency of O—H stretching in phenol (proton donor)–BDMA (borane-dimethylamine) complex has been reported to show a red shift by 174 cm^{-1} when the dihydrogen bonding forms (37). Likewise, the N—H stretching in the complex between 2-pyridone (as the proton donor) and borane-trimethylamine also shows a red shift by 5 cm^{-1} upon the formation of dihydrogen (37). Other than in those compounds, we have observed that the N—H stretching frequency of lithium amidoborane is blue shifted relative to its parent compound (Fig. 1), which indicates that either the dihydrogen bonding becomes weaker compared with ammonia borane or it disappears in lithium amidoborane structure.

Existence of dihydrogen bonding shows unique behavior at high pressure. According to Lipincott's model (38), existence of N—$H^{\delta+}$... $H^{\delta-}$—B dihydrogen bonding (Fig. 4) in the structure will result in a large redshift in the N—H stretching frequencies as the N...$H^{\delta-}$ (intermolecular) distance decreases. The $H^{\delta+}$...$H^{\delta-}$ dihydrogen bonding strengthens in the N—$H^{\delta+}$...$H^{\delta-}$—B configuration, with the sacrifice of N—$H^{\delta+}$ bond strength. That is, as the intermolecular (N...$H^{\delta-}$) distance decreases, the N—$H^{\delta+}$ bond length increases; therefore, the N—$H^{\delta+}$ restoring force decreases, i.e., the frequency shifts to lower wavenumbers. Applying external pressure is a mean to decrease the intermolecular N...$H^{\delta-}$ distance. So, if there is any dihydrogen bonding in the material, the N—H stretching should exhibit redshift with pressure (25–27, 30) with some exceptions that have very strong symmetric dihydrogen bonding (39–46). As shown in Fig. 3 *B* and *C*, the N—H stretching frequency of lithium amidoborane shows blue shift with increasing pressure, in contrast to its parent compound ammonia borane (25–27, 30). The observation of blueshift of N—H stretching frequency with pressure indicates a likely absence of dihydrogen bond in lithium amidoborane as illustrated by Lipincott's model, unless there is an extremely strong symmetric dihydrogen bonding. Cambridge Structural Database (CSD) structural search provides characteristic metric data for 26 N—H...H—B intermolecular dihydrogen bonds with H...H distance in the range of 1.7–2.2 Å in 18 crystal structures (47–50). X-ray diffraction data, however, indicate that the NH... HB intermolecular distance of lithium amidoborane is 2.249 Å (18), 10% longer than that of ammonia borane (2.02 Å) (18) and close to the expected van der Waals distance (2.4 Å). This fact may rule out the possibility of extremely strong dihydrogen bonding in lithium amidoborane.

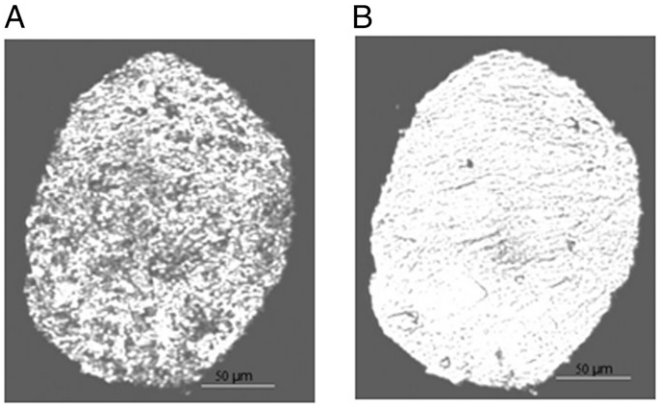

Fig. 3. Change of photomicrograph of lithium amidoborane in gasket hole associated with the first phase transition at 2.4 GPa (before first phase transition; *A*) and 3.9 GPa (after the first phase transition; *B*).

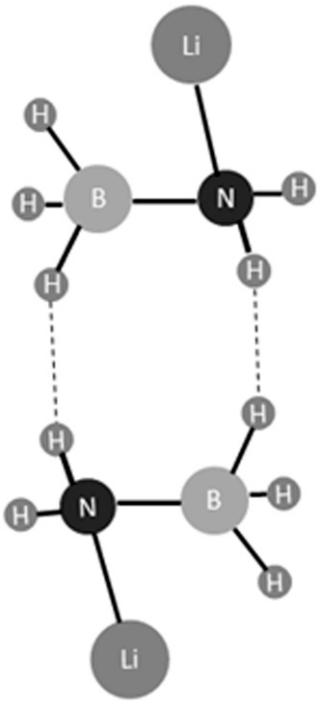

Fig. 4. Schematic structure of two molecules of $LiNH_2BH_3$. The dashed line indicates the location of the possible dihydrogen bonding.

The Li-N bond length of $LiNH_2BH_3$, ~2.032 Å (15, 51, 52), is significantly longer than the H—N bond length (1.07 Å) in ammonia borane (52, 53). Each Li^+ is tetrahedrally surrounded by three other $BH_3^{\delta-}$ units with the experimentally determined Li...B distance of 2.50–2.69Å (18) and theoretically predicted Li...B distance of 2.564–2.646 Å (32). As lithium is more electron-donating, N attracts more electrons from lithium than the hydrogen atoms. So, N—H bond approaches to the covalent character (i.e., its bond length decreases), whereas Li—N shows more ionic character. So, there may be significant van der Waals interaction between Li^+... $BH_3^{\delta-}$, which acts as the stabilizing factor for the molecular structure of $LiNH_2BH_3$ although the dihydrogen bonding is absent in its structure. The absence of the dihydrogen bonding not only alters the structure stabilizing factor of $LiNH_2BH_3$, it may also cause significant change in the dehydrogenation mechanism of this complex. In principle, the

attractive interaction between the dihydrogen bonded atoms strongly lowers the activation energy for hydrogen release of ammonia borane (37, 54, 55) and also some potential complexes for hydrogen storage (53). Although there is no dihydrogen bond, $LiNH_2BH_3$ dehydrogenates at lower temperature than ammonia borane, which refers to a different dehydrogenation mechanism other than mere $H^{\delta+}...H^{\delta-}$ interaction mechanism claimed by Chen et al. (15). As B—H bond is weaker in lithium amidoborane, B—H shows more reactivity in dehydrogenation and the transfer of hydrogen from boron to lithium is the rate-determining step of dehydrogenation process of lithium amidoborane (56, 57). It will open new opportunities for the design of hydrogen storage material by tuning the reactivity of N—H and/or B—H by substituting protonic and/or hydridic hydrogen by more electroposive and/or electronegative elements. If both of the N—H and B—H bonding can be made weaker by simultaneously substituting protonic and hydridic hydrogen, then dihydrogen bonding may appear in the structure, which may dehydrogenate more easily than metal amidoboranes.

Materials and Methods

Sample Preparation in Capillary. $LiNH_2BH_3$ and NH_3BH_3 were purchased from Sigma Aldrich with stated purities of 90% and 97%, respectively, and were used without further purification. Due to air sensitivity of lithium amidoborane, all sample handlings were done inside an argon-filled glovebox. The sample was loaded into a capillary inside the glovebox and then sealed.

DAC Sample Preparation. A symmetric DAC with two type-I diamonds of 400 μm culet size was used for the high-pressure experiments. A stainless steel gasket was preindented to 55 μm thickness and then a hole of 160 μm in diameter was drilled in the center as a sample chamber. Lithium amidoborane powders, along with some ruby chips for in situ pressure measurement, were loaded in the sample chamber inside the glovebox. Pressure was calibrated from the shift of Ruby fluorescence (58, 59). No pressure medium was used in the sample chamber as the sample is fairly soft.

Raman Spectroscopy Measurements. Raman spectroscopy measurements were conducted in the Center for the Study of Matter at Extreme Condition (CeSMEC) at Florida International University. This system uses a 514-nm Ar^+ laser excitation line and has 2 cm^{-1} spectra resolution.

Optical Microscope Measurement. Direct microscopic observation through diamond windows were recorded before and after the first phase transition.

Conclusion

Raman spectroscopy was used to investigate the bonding behavior of lithium amidoborane structure and the phase stability of lithium amidoborane at high pressure and room temperature. In the lithium amidoborane structure, the bonding behavior is significantly altered from its parent compound ammonia borane. The characteristic dihydrogen bonding of ammonia borane is absence in lithium amidoborane. This phenomenon is evidenced by the blueshift of N—H stretching frequency compared with its parent compound ammonia borane in the ambient condition Raman spectra along with the positive pressure dependence of N—H stretching frequency of lithium amidoborane at high pressure observed in this experiment. Also, B—H bonding becomes weaker in lithium amidoborane structure, which will show more reactivity in dehydrogenation. The different bonding characteristics are likely responsible for improved dehydrogenation behavior of lithium amidoborane. The Raman spectroscopy study and optical microscopy study identified two phase transitions of lithium amidoborane at high pressure and room temperature. The first phase transition occurs at 3.9 GPa and the second phase transition occurs at 12.7 GPa. These new phases are likely to have more volumetric hydrogen content. Future X-ray and neutron diffraction study is required to further investigate the phase transition and the absence of dihydrogen bonding.

ACKNOWLEDGMENTS. We thank Dr. Surendra K. Saxena, Dr. Vadym Drozd, and Dr. Andriy Durygin for their technical support. This work was supported by the US Department of Energy (DOE) under Award DE-FG02-07ER46461. We thank EFree, an Energy Frontier Research Center funded by the US DOE, Office of Science, and Office of Basic Energy Sciences under Award DE-SC0001057 for partial personnel support.

1. Schlapbach L, Züttel A (2001) Hydrogen-storage materials for mobile applications. *Nature* 414(6861):353–358.
2. Chen P, Zhu M (2008) Recent progress in hydrogen storage. *Mater Today* 11:36–43.
3. Graetz J (2009) New approaches to hydrogen storage. *Chem Soc Rev* 38(1):73–82.
4. Irvine J (2008) Theme issue: Materials chemistry for hydrogen storage and generation. *J Mater Chem* 18:2295–2297.
5. Felderhoff M, Weidenthaler C, von Helmolt R, Eberle U (2007) Hydrogen storage: The remaining scientific and technological challenges. *Phys Chem Chem Phys* 9(21): 2643–2653.
6. Bowden M, Autrey T, Brown I, Ryan M (2008) The thermal decomposition of ammonia borane: A potential hydrogen storage material. *Curr Appl Phys* 8:498–500.
7. Baitalow F, Baumann J, Wolf G, Jaenicke-Rössler K, Leitner G (2002) Thermal decomposition of B–N–H compounds investigated by using combined thermoanalytical methods. *Thermochim Acta* 391:159–168.
8. Wolf G, Baumann J, Baitalow F, Hoffmann FP (2000) Calorimetric process monitoring of thermal decomposition of B-N-H compounds. *Thermochim Acta* 343:19–25.
9. Gutowska A, et al. (2005) Nanoscaffold mediates hydrogen release and the reactivity of ammonia borane. *Angew Chem Int Ed Engl* 44(23):3578–3582.
10. Bluhm ME, Bradley MG, Butterick R, 3rd, Kusari U, Sneddon LG (2006) Amineborane-based chemical hydrogen storage: Enhanced ammonia borane dehydrogenation in ionic liquids. *J Am Chem Soc* 128(24):7748–7749.
11. Stephens FH, Baker RT, Matus MH, Grant DJ, Dixon DA (2007) Acid initiation of ammonia-borane dehydrogenation for hydrogen storage. *Angew Chem Int Ed Engl* 46 (5):746–749.
12. Keaton RJ, Blacquiere JM, Baker RT (2007) Base metal catalyzed dehydrogenation of ammonia-borane for chemical hydrogen storage. *J Am Chem Soc* 129(7):1844–1845.
13. Jaska CA, Temple K, Lough AJ, Manners I (2003) Transition metal-catalyzed formation of boron-nitrogen bonds: Catalytic dehydrocoupling of amine-borane adducts to form aminoboranes and borazines. *J Am Chem Soc* 125(31):9424–9434.
14. Hamilton CW, Baker RT, Staubitz A, Manners I (2009) B-N compounds for chemical hydrogen storage. *Chem Soc Rev* 38(1):279–293.
15. Xiong Z, et al. (2008) High-capacity hydrogen storage in lithium and sodium amidoboranes. *Nat Mater* 7(2):138–141.
16. Kang X, et al. (2008) Ammonia borane destabilized by lithium hydride: An advanced on-board hydrogen storage material. *Adv Mater (Deerfield Beach Fla)* 20:2756–2759.
17. Chua YS, Chen P, Wu G, Xiong Z (2011) Development of amidoboranes for hydrogen storage. *Chem Commun (Camb)* 47(18):5116–5129.
18. Wu H, Zhou W, Yildirim T (2008) Alkali and alkaline-earth metal amidoboranes: structure, crystal chemistry, and hydrogen storage properties. *J Am Chem Soc* 130(44): 14834–14839.
19. Diyabalanage HVK, et al. (2007) Calcium amidotrihydroborate: A hydrogen storage material. *Angew Chem Int Ed* 46:8995–8997.
20. Diyabalanage HVK, et al. (2010) Potassium(I) amidotrihydroborate: Structure and hydrogen release. *J Am Chem Soc* 132(34):11836–11837.
21. Xiong Z, et al. (2008) Synthesis of sodium amidoborane (NaNH2BH3) for hydrogen production. *Energy Environ Sci* 1:360–363.
22. Mao WL, Mao HK (2004) Hydrogen storage in molecular compounds. *Proc Natl Acad Sci USA* 101(3):708–710.
23. Mao WL, Koh CA, Sloan ED (2007) Clathrate hydrates under pressure. *Phys Today* 60(10):42–47.
24. Mao WL, et al. (2002) Hydrogen clusters in clathrate hydrate. *Science* 297(5590): 2247–2249.
25. Trudel S, Gilson DFR (2003) High-pressure Raman spectroscopic study of the ammonia-borane complex. Evidence for the dihydrogen bond. *Inorg Chem* 42(8):2814–2816.
26. Custelcean R, Dreger ZA (2003) Dihydrogen bonding under high pressure: A raman study of $BH3NH_3$ molecular crystal. *J Phys Chem B* 107:9231–9235.
27. Lin Y, Mao WL, Drozd V, Chen J, Daemen LL (2008) Raman spectroscopy study of ammonia borane at high pressure. *J Chem Phys* 129(23):234509.
28. Chellappa RS, Somayazulu M, Struzhkin VV, Autrey T, Hemley RJ (2009) Pressure-induced complexation of NH_3BH_3–H_2. *J Chem Phys* 131:2245151–2245159.
29. Chen J, et al. (2010) In situ X-ray study of ammonia borane at high pressures. *Int J Hydrogen Energy* 35:11064.
30. Xie S, Song Y, Liu Z (2009) In situ high pressure study of ammonia borane by Raman and IR spectroscopy. *Can J Chem* 87:1235–1247.
31. Ryan KR, et al. (2011) A combined experimental inelastic neutron scattering, Raman and *ab initio* lattice dynamics study of α-lithium amidoborane. *Phys Chem Chem Phys* 13(26):12249–12253.
32. Lee SM, Kang XD, Wang P, Cheng HM, Lee YHA (2009) A comparative study of the structural, electronic, and vibrational properties of NH3BH3 and LiNH2BH3: Theory and experiment. *ChemPhysChem* 10(11):1825–1833.
33. Ramzan M, et al. (2009) Structural and energetic analysis of the hydrogen storage materials $LiNH_2BH_3$ and $NaNH_2BH_3$ from *ab initio* calculations. *Phys Rev B* 79: 1321021–1321024.

34. Cai-Lin L, et al. (2010) Structures and stability of metal amidoboranes (MAB): density functional calculations. *Commun Theor Phys* 53:1167–1171.
35. Armstrong DR, Perkins PG, Walker GT (1985) The electronic structure of the monomers, dimers, a trimer, the oxides and the borane complexes of the lithiated ammonias. *J Mol Struct THEOCHEM* 122:189–204.
36. Kar T, Scheiner S (2003) Comparison between hydrogen and dihydrogen bonds among H_3BNH_3, H_2BNH_2, and NH_3. *J Chem Phys* 119:1473–1482.
37. Fujii A, Patwari GN, Ebata T, Mikami N (2002) Vibrational spectroscopic evidence of unconventional hydrogen bonds. *Int J Mass Spectrom* 220:289–312.
38. Lippincott ER, Schroeder R (1955) One-dimensional model of the hydrogen bond. *J Chem Phys* 23:1099–1106.
39. Moon SH, Drickamer HG (1974) Effect of pressure on hydrogen bonds on organic solids. *J Chem Phys* 61:48–54.
40. Hamann SD, Linton M (1975) The influence of pressure on the Infrared spectra of hydrogen-bonded solids. I Compounds with O-H. . . O Bonds. *Aust J Chem* 28: 2567–2578.
41. Hamann SD, Linton M (1976) The influence of pressure on the Infrared spectra of hydrogen-bonded solids. II Bihalide salts. *Aust J Chem* 29:479–484.
42. Hamann SD, Linton M (1976) The influence of pressure on the Infrared spectra of hydrogen-bonded solids. III Compounds with N-H. . .X Bonds. *Aust J Chem* 29: 1641–1647.
43. Hamann SD, Linton M (1976) The influence of pressure on the Infrared spectra of hydrogen-bonded solids. IV Miscellaneous compounds. *Aust J Chem* 29:1825–1827.
44. Hamann SD (1977) The influence of pressure on the infrared spectra of hydrogen-bonded solids. V The formation of fermi resonance 'windows'. *Aust J Chem* 30:71–79.
45. Hamann SD (1978) The influence of pressure on the Infrared spectra of hydrogen-bonded solids. VI Ammonium salts. *Aust J Chem* 31:11–18.
46. Hamann SD (1988) The influence of pressure on the Infrared spectra of hydrogen-bonded solids. VII Deuterated ammonium salts. *Aust J Chem* 41:1935–1941.
47. Crabtree RH, Siegbahn PEM, Eisenstein O, Rheingold AL, Koetzle TF (1996) A new intermolecular interaction: Unconventional hydrogen bonds with element-hydride bonds as proton acceptor. *Acc Chem Res* 29(7):348–354.
48. Klooster WT, Koetzle TF, Siegbahn PEM, Richardson TB, Crabtree RH (1999) Study of the N-H. . .H-B dihydrogen bond including the crystal structure of BH_3NH_3 by Neutron diffraction. *J Am Chem Soc* 121:6337–6343.
49. Richardson TB, Gala SD, Crabtree RH (1995) Unconventional hydrogen bonds: Intermolecular B-H. . .H-N interactions. *J Am Chem Soc* 117:12875–12876.
50. Richardson TB, Koetzle TF, Crabtree RH (1996) An M-H. . .H-C hydrogen bonding interaction. *Inorg Chim Acta* 250:69–73.
51. Wu C, et al. (2010) Stepwise phase transition in the formation of lithium amidoborane. *Inorg Chem* 49(9):4319–4323.
52. Hoon CF, Reynhardt E (1983) Molecular dynamics and structures of amine boranes of the type R_3N BH_3: I. X-ray investigation of $H_3N.BH_3$ at 295 K and 110 K. *J Phys C Solid State Phys* 16:6129–6136.
53. Li W, et al. (2010) Understanding from first-principles why $LiNH_2BH_3{\cdot}NH_3BH_3$ shows improved dehydrogenation over $LiNH_2BH_3$ and NH_3BH_3. *J Phys Chem C* 114:19089–19095.
54. Grochala W, Edwards PP (2004) Thermal decomposition of the non-interstitial hydrides for the storage and production of hydrogen. *Chem Rev* 104(3):1283–1316.
55. Lu J, Fang ZZ, Sohn HY (2006) A dehydrogenation mechanism of metal hydrides based on interactions between Hdelta+ and H-. *Inorg Chem* 45(21):8749–8754.
56. Swinnen S, Nguyen VS, Nguyen MT (2010) Potential hydrogen storage of lithium amidoboranes and derivatives. *Chem Phys Lett* 489:148–153.
57. Kim DY, Lee HM, Seo J, Shin SK, Kim KS (2010) Rules and trends of metal cation driven hydride-transfer mechanisms in metal amidoboranes. *Phys Chem Chem Phys* 12(20): 5446–5453.
58. Mao HK, Bell PM (1978) Specific volume measurements of Cu, Mo, Pd, and Ag and calibration of the ruby R_1 fluorescence pressure gauge from 0.06 to 1 Mbar. *J Appl Phys* 49:3276–3283.
59. Mao HK, Xu J, Bell PM (1986) Calibration of the ruby pressure gauge to 800 kbar under quasi-hydrostatic conditions. *J Geophys Res* 91:4673–4676.